ACOUSTIC SURFACE WAVE PROBING OF CERAMICS

J. Tien, B. Khuri-Yakub, and G. S. Kino
Stanford University
Stanford, California 94305

ABSTRACT

We have developed a low frequency theory for scattering from surface cracks. For the case of half-penny shaped surface cracks, we are able to relate the reflection coefficient of a Rayleigh wave incident on the crack with the crack size as well as the fracture stress of a sample with the crack in it. Comparisons of the theoretical predictions for the fracture stress with the actual fracture stresses for silicon nitride samples containing cracks with estimated radii ranging from 51 μm to 274 μm show excellent agreement, with less than 16% error. A qualitative study in the high frequency regime of the reflected echos from surface cracks in silicon nitride turbine blades has also been made.

INTRODUCTION

Our aim in this work has been to establish qualitative and quantitative procedures for identifying cracks in the surface of structural ceramics. The basic technique we have been employing is to excite a Rayleigh wave on the surface of the ceramic and observe reflections of the acoustic surface wave from the crack. Accordingly, we have developed techniques for exciting acoustic waves in the low frequency range below 10 MHz and another range of experimental methods for exciting acoustic waves at frequencies above 50 MHz . As we are interested in cracks ranging in size from 25 μm upwards and the wavelengths at 10 MHz and 50 MHz are typically 600 μm and 120 μm , respectively, both these low and high frequency techniques are important.

Currently, most of the quantitative studies have been carried out in the low frequency regime because here we have been able to develop in detail a theory to associate our experimental measurements with not only the crack size but also with the fracture stress of a sample with a crack present. Such an association can be made because the stress field due to a Rayleigh wave has a component of longitudinal stress parallel to the surface for penetration depths much less than an acoustic wavelength and consequently, the fields in the neighborhood of a crack are distorted in the same way as they would be for an applied static stress (i.e., a bending stress) where the acoustic wavelength is much larger than a typical crack dimension. It is thus possible to establish a relation between the reflection coefficient of the Rayleigh wave (which one can obtain via acoustic measurements) and the stress intensity factor. Knowing the stress intensity factor then allows us to predict the fracture stress of a sample when the crack is present.

THEORETICAL DEVELOPMENTS

The theory we describe here has its restrictions in that it requires the depth to which the crack extends below the sample surface to be less than a tenth of the acoustic wavelength. This, however, implies that the signal reflected back from a crack is very weak. The simple theory we will begin with is based on the idea that the fields in the neighborhood of a half-penny shaped surface crack can be calculated by assuming that they are distorted in approximately the same way as the fields in the neighborhood of a circular volume crack. This, in fact, is not an entirely adequate assumption because the stresses are changed near the surface for a semi-circular crack, and the stress intensity factor tends to be higher near the surface of a material than in its interior. Furthermore, the Rayleigh wave fields are not uniform across the plane of the crack, but rather, fall off with depth into the sample. We will take these modifications into account in a later part of our theory. Lastly, we will discuss briefly the effect on the results should the crack be semi-elliptical rather than semi-circular.

Kino and Auld have worked out a general theory of scattering from flaws.[1,2] The situation considered is illustrated in Fig. 1. Transducer 1 transmits a signal with amplitude A_1 . This signal is reflected off the flaw and the reflected wave is received by transducer 2. The reflection coefficient S_{21} is defined as the amplitude ratio of the reflected signal A_2 , to the incident signal A_1 , at the terminals of the transducers and is given by the relation

$$S_{21} \equiv \frac{A_2}{A_1} = \frac{j\omega}{4P_1} \int_{S_c} u_j^{(2)} \sigma_{ij}^{A(1)} n_i dS \qquad (1)$$

Here, P_1 is the input power to the transmitting transducer, $u_j^{(2)}$ is the Rayleigh wave displacement field when the receiving transducer is used as the transmitter, and $\sigma_{ij}^{A(1)}$ is the applied stress in the vicinity of the flaw before the flaw has been introduced. The integral here is taken over the entire surface of the flaw, S_c . When the same transducer is used to both transmit and receive, we write $S_{21} = S_{11}$.

We will begin by considering the case of a Rayleigh wave normally incident on a half-penny shaped crack located in the x-y plane (Fig. 2). The reflection coefficient then may be written as

$$S_{11} = \frac{j\omega}{4P_1} \int_S \Delta u_z \sigma_{zz}^A dS \qquad (2)$$

where now Δu_z is the discontinuity in the Rayleigh wave displacement field across the crack, and

σ^A_{zz} is the applied stress. The integral is taken over just the semi-circular area, S. To evaluate the displacement discontinuity, Δu_z, we initially use the theory for a penny-shaped crack of radius a.[3] This gives the result

$$\Delta u_z = k_I \sigma^A_{zz} \frac{4}{(\pi a)^{1/2}} \frac{1 - \nu^2}{E} (a^2 - r^2)^{1/2} \qquad (3)$$

where $k_I = 2(a/\pi)^{1/2}$ is the normalized mode I stress intensity factor, E is Young's modulus, ν is Poisson's ratio, and r is the distance from the center of the crack. Using Eq. (3) in Eq. (2) and approximating the stress σ^A_{zz} by its value at the sample surface, namely $\sigma^A_{zz}|_{surf}$, we find for the reflection coefficient

$$S_{11} = \frac{2}{3} j\omega \frac{(\sigma^A_{zz}|_{surf})^2}{P_1} a^3 \frac{(1 - \nu^2)}{E} \qquad (4)$$

Note the cubic dependence of the reflection coefficient on the crack radius a. Evaluating $\sigma^A_{zz}|_{surf}$ in terms of the input power P_1 gives then for the modulus of S_{11}

$$|S_{11}| = \frac{16\pi^2}{3} \frac{f_z \eta a^3}{\lambda^2 w(1 - \nu)} \equiv R \qquad (5)$$

In Eq. (5), f_z is a material's parameter tabulated by Auld,[4] η is a loss term, λ is the acoustic wavelength, and w is the width of the incident beam. Typically, for a ceramic with a Poisson's ratio $\nu \simeq 0.2$, $f_z \simeq 0.4$.

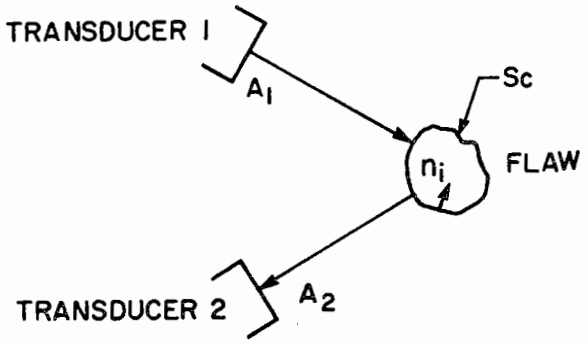

Fig. 1. A schematic of the geometry considered in the derivation of the reflection coefficient, S_{21}, for a flaw.

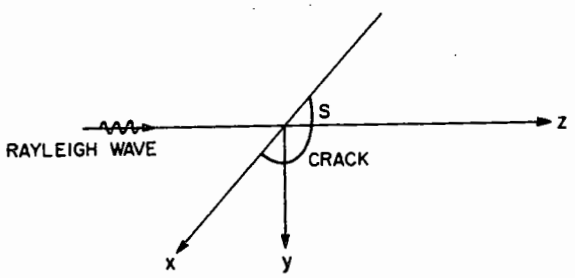

Fig. 2. Scattering geometry for Rayleigh wave normally incident on a half-penny shaped crack.

For a crack located on the central axis of the beam, the loss term η can be written as

$$\eta = \eta_T \eta_D \qquad (6)$$

where η_T is the transducer power loss in converting the input electrical signal to an acoustic surface wave and η_D is a diffraction loss term. For a crack a distance z from the transducer located in the far field of the transducer, i.e., for $z > w^2/\lambda$, η_D may be expressed as

$$\eta_D = w^2/\lambda z \qquad (7)$$

More generally, an effective value for η_D can be calculated by averaging the stress field over the width of the transducer. The result is shown in Fig. 3. We observe that for $z > w^2/\lambda$ (far field region), the formula given for η_D in Eq. (7) is indeed accurate.

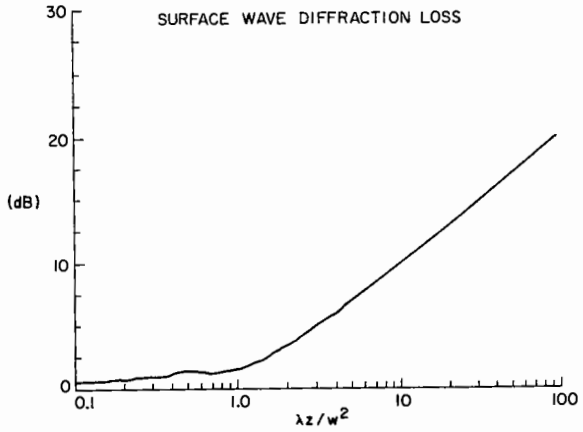

Fig. 3. Surface wave diffraction loss as a function of the normalized distance from the transducer, $\lambda z/w^2$.

We next modify the theory to take into account scattering from the crack at an angle. We consider the case where the transmitting transducer 1 produces an acoustic wave incident on the crack at an angle θ with respect to the crack normal and the receiving transducer 2 receives the reflected wave at an angle $-\theta$ (Fig. 4A). A simplification of this situation occurs when a single transducer is used to both transmit and receive along a line at an angle θ with respect to the crack normal (Fig. 4B). This second configuration is of interest in considering backscatter from a crack at an arbitrary angle. One problem, however, that we have encountered experimentally when using the same transducer to both transmit and receive is that spurious signals are produced by the transducer which tend to interfere with the reflected signals received. This is especially troublesome when the reflected signals are very weak. In such situations, the first configuration (Fig. 4A) becomes useful as the receiving transducer then receives only the acoustic wave reflected off the crack and none of the spurious signals produced by the transmitting transducer.

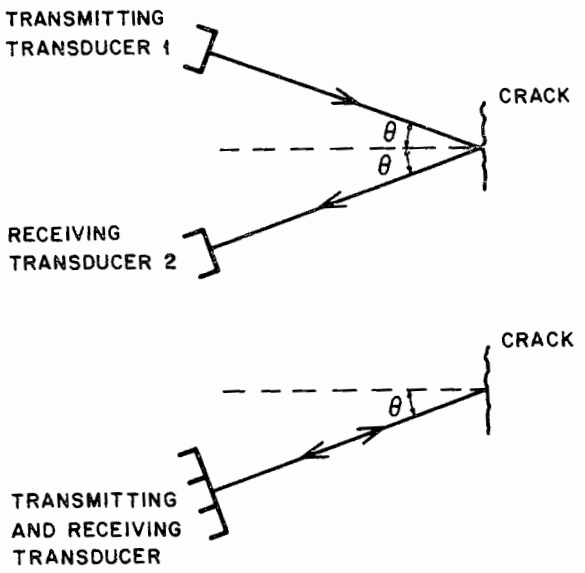

Fig. 4. (A) Two-transducer configuration and (B) single transducer configuration for scattering from the crack at an angle.

For each of these configurations, we find that the reflection coefficients are given by

$$|S_{21}| = R|G(\theta)| \quad \text{two-transducer configuration} \tag{8A}$$

$$|S_{11}| = RF(\theta) \quad \text{single transmitting and receiving transducer} \tag{8B}$$

where

$$\begin{Bmatrix} G(\theta) \\ F(\theta) \end{Bmatrix} = (\cos^2\theta - \nu \sin^2\theta)^2 = \frac{(1+\nu)^2}{2(2-\nu)} \sin^2 2\theta \tag{9}$$

and R is defined in Eq. (5). Examples of the angular variation of $F(\theta)$ and $|G(\theta)|$ for the case of silicon nitride are shown in Figs. 5 and 6. Note that neither $F(\theta)$ nor $|G(\theta)|$ vanish at $\theta = 90°$.

We now discuss how imaging forces at the surface, which affect the value of the stress intensity factor near the surface, and the variation with depth of the Rayleigh wave stress fields can be taken into account for the case of scattering at normal incidence from a half-penny shaped crack. Again, the reflection coefficient is given by Eq. (2). It has been shown by Budiansky and O'Connell[5] that the surface integral given in Eq. (2) is related to the crack formation energy, $\mathcal{E}$, by

$$= (1/2)\int_S \Delta u_z \sigma_{zz}^A dS \tag{10}$$

Alternatively, $\mathcal{E}$ may be written as

$$= \frac{1-\nu^2}{3E} \int_C a K_I^2(\tilde{\theta}) d\ell \tag{11}$$

where C is the crack circumference shown in Fig. 7. Due to the surface imaging forces, the stress intensity factor is a function of the angle $\tilde{\theta}$, taken to be the angle from the normal to the sample surface passing through the crack center. To evaluate the angular dependence of K_I, we make use of a theory by Smith, Emery, and Kobayashi.[6] Smith, et al. considered the case of a half-penny shaped crack in a plate of thickness $2c$, to which a bending stress was applied. The applied stress then has a linear form given by

$$\sigma_{zz}^A(y) = A(1 - y/c) \tag{12}$$

where A is a constant, and y is the distance from the surface of the substrate. The stress intensity factor is consequently given by

$$K_I(\tilde{\theta}) = 2\sqrt{a/\pi}\, A\, [\psi_0(\tilde{\theta}) - (a/c)\psi_1(\tilde{\theta})] \tag{13}$$

where $\psi_0(\tilde{\theta})$ and $\psi_1(\tilde{\theta})$ were numerically evaluated by Smith et al. and are shown in Fig. 8. Here, the function $\psi_0(\tilde{\theta})$ determines the increase in the stress intensity factor near the sample surface and the quantity $-(a/c)\psi_1(\tilde{\theta})$ governs the fall-off in the Rayleigh wave stress field with depth. To evaluate the effective values for the constants A and c for our case where the stress, is due to the Rayleigh wave and not a bending stress we determine the exact variation of the stress field with depth y, following the work of Viktorov,[7] and make a linear approximation. The result for silicon nitride is shown in Fig. 9. Note that the linear approximation follows the exact curve very well for $y/\lambda < 0.1$. With this approximation, we can find A and c in terms of the surface value of the stress σ_{zz}^A and the slope of the linear approximation. Evaluating $K_I(\tilde{\theta})$, substituting the results into Eq. (11), and using Eqs. (2) and (10) then gives for the reflection coefficient

$$|S_{11}| = R\, H(\tfrac{2\pi a}{\lambda}) \tag{14}$$

where $H(2\pi a/\lambda)$ must be numerically evaluated and is plotted in Fig. 10 for the case of silicon nitride. Observe that there is a considerable reduction in the scattering amplitude as the value of the parameter $2\pi a/\lambda$ increases. In view of the linear approximation we have made, we normally would expect this theory to be accurate for values of $2\pi a/\lambda$ less than unity; however, we have found that the theory does surprisingly well even for much larger values of this parameter.

The theory by Smith et al. has also been used by us in collaboration with Resch[8] to predict the maximum measured stress intensity factor for semi-elliptical cracks, using a formulation very similar to that already given. In the interests of brevity, we will not go into the details of these results here. Suffice it to say that the measured stress intensity factor varies by a factor of 1.22 to .8 as the ratio of the minor to major axes varies from 1 to 0.1. Thus, the variation is somewhat larger than that predicted by Budiansky and Rice.[9] On the other hand, when considering surface cracks in brittle materials such as ceramics or glasses, the variation of the ratio of minor to major axes typically ranges only from 1.0 to 0.5, with the corresponding variation in the stress intensity factor going from 1.22 to 1.05.

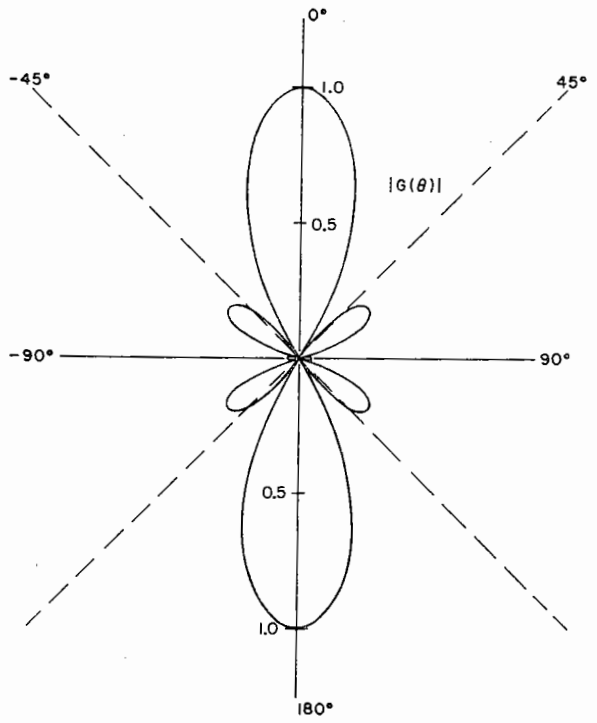

Fig. 5. Angular variation of $|G(\theta)|$, which determines the angular dependence of the reflection coefficient for the two-transducer configuration, for the case of silicon nitride.

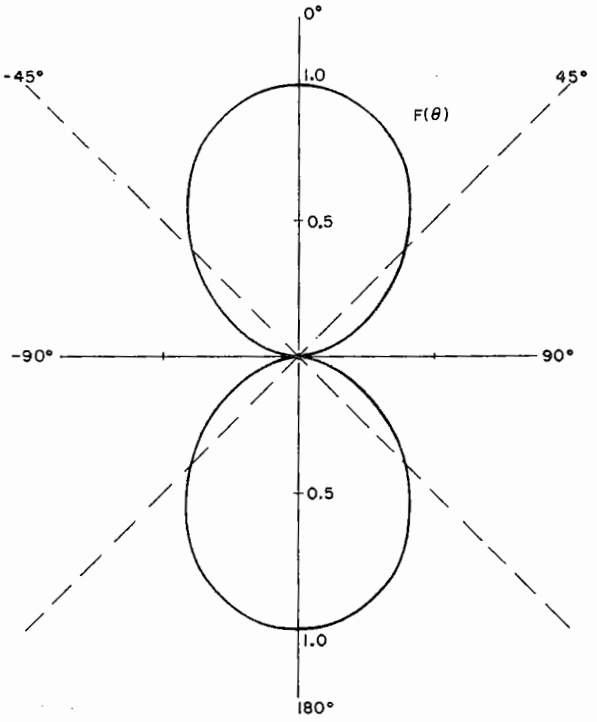

Fig. 6. Angular variation of $F(\theta)$, which determines the angular dependence of the reflection coefficient for the single transducer configuration, for the case of silicon nitride.

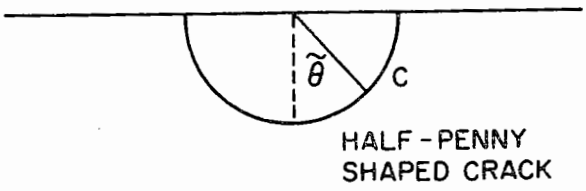

Fig. 7. Schematic of half-penny shaped crack geometry.

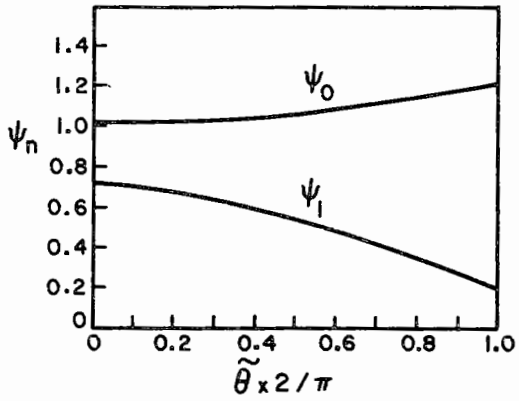

Fig. 8. Functions $\psi_0(\tilde{\theta})$ and $\psi_1(\tilde{\theta})$ vs. $\tilde{\theta}$ numerically evaluated by Smith, Emery, and Kobayashi.[6]

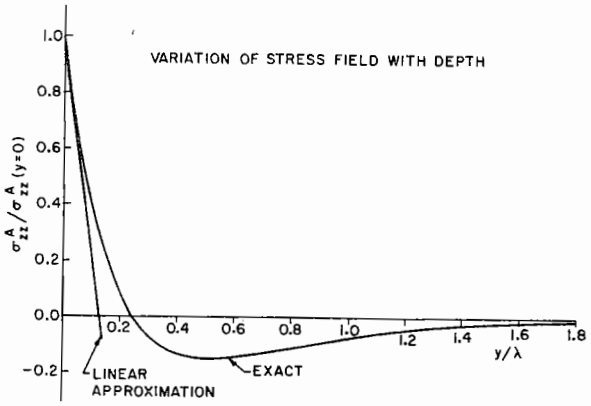

Fig. 9. Variation of stress field with depth in both exact form and in linear approximation for the case of silicon nitride.

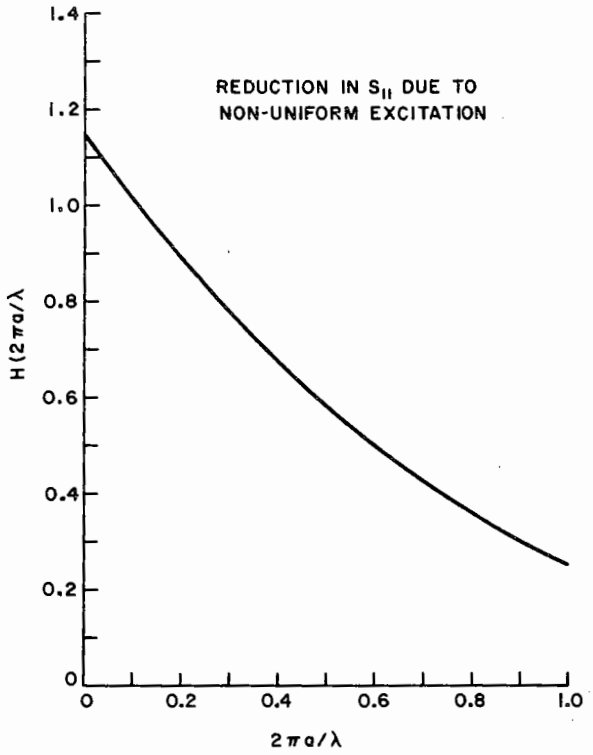

Fig. 10. Reduction in $|S_{11}|$ due to surface imaging forces and depth variation in the Rayleigh wave stress field for the case of silicon nitride.

QUANTITATIVE MEASUREMENTS ON FLAT SURFACES

We discuss here the quantitative measurements we have made in the low frequency regime. The ceramic selected for this study was a commercial hot-pressed silicon nitride (NC-132). Plate specimens (7.6 × 2.6 × .64 cm) were machined from an as-pressed billet and the surfaces optically polished. Cracks were introduced into each sample using a Knoop hardness indentor by Evans at Berkeley and Resch at Stanford.

In our experiments, we used a wedge transducer to excite a Rayleigh wave on the surfaces of the samples as shown in Fig. 11. We carried out a series of measurements on different sizes of cracks using both the technique of direct backscatter to a single transducer acting as both the transmitter and receiver as well as the technique employing two different transducers, one to transmit and the other to receive. Our measurements were made at a frequency of about 9 MHz , which corresponds to an acoustic wavelength of about 650 μm . The results are shown in Table I. Note that the parameter $2\pi a/\lambda$ is well within the range we expect our theory to be accurate for the smaller 5 kg and 10 kg cracks but is well out of this range for the larger 20 kg cracks. From our estimates for the crack radii, we were able to predict a value for the fracture stress $\sigma_F^{Acoustic}$ by using the relation

$$\sigma_F^{Acoustic} = \frac{K_{IC}}{k_I\big|_{surf}} \qquad (15)$$

where

$$k_I\big|_{surf} = 1.22\, k_I\big|_{bulk} = 1.22[2(a/\pi)^{1/2}] \qquad (16)$$

and $K_{IC} = 3.55$ MPa$\sqrt{m}$.[10] We then broke the samples and measured the actual fracture stress. The deviations between the predicted values and the actual values of the fracture stress are shown in the last column of Table I. In all cases, the error in our measurements is less than 16%, with the measurements on the smaller cracks having the best accuracy, as anticipated.

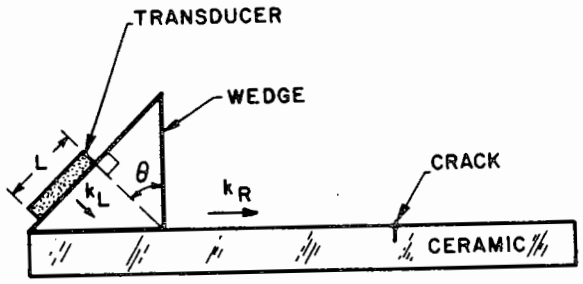

Fig. 11. Schematic of surface crack and experimental set up.

TABLE 1

Sample	Acoustic a (μm)	$2\pi a/\lambda$	Acoustic σ_F (MPa)	Actual σ_F (MPa)	%
5 kg: 1	56	.5391	350	338.45	3.3
2	51	.4960	367	365	.54
10 kg: 1	67	.6493	320	298.5	6.72
2	66	.6396	322.7	275.4	14.6
20 kg: 1	274	2.650	158.4	159.22	.52
2	262	2.539	159.7	179.13	12.17
3	255	2.470	164.2	189	15.1

We also made a preliminary study to determine whether the cracks in our samples might be partially closed. To do this, we applied a calibrated bending stress to the sample while simultaneously measuring the reflected signal from the crack. We found that our estimate of the crack radius tended to increase by about 10% from its unstressed value under the application of a bending stress. We thus conclude that the cracks in our samples were indeed partially closed when the samples were in an unstressed state.

MEASUREMENTS ON TURBINE BLADE ROOTS

The silicon nitride turbine blades used in this study were manufactured by Airesearch Manufacturing Co. and provided to us by H. G. Graham from AFML. A schematic of a turbine blade and the experimental set-up is shown in Fig. 12. Our aim in this study was to detect and locate cracks in the neck region of the turbine blades. In Fig. 12, the $LiNbO_3$ transducer was used as both the transmitter and the receiver. Experiments were carried out at both

64 MHz and 100 MHz. In our initial study, all six turbine blades supplied to us gave indications that either cracks or machining marks were present in the neck region. In Fig. 13A, we show a picture taken with an optical microscope of the neck region. Here, the presence of machining marks with a periodicity of about 20 μm is clearly indicated. As we expect the depth b of the machining marks to be no greater than about 25 μm, we can determine the reflection coefficient from these marks by assuming $\lambda >> b$ and using a long wavelength theory. Making assumptions regarding the stress fields similar to those initially made in our simple theory for the half-penny shaped crack and approximating the geometry of a machining mark by a long slit crack, we find that

$$|S_{11}| = C(\nu)\eta \frac{b^2}{\lambda^2} \qquad (17)$$

Here, η is again a loss term and $C(\nu) \approx 8.694$ for silicon nitride.

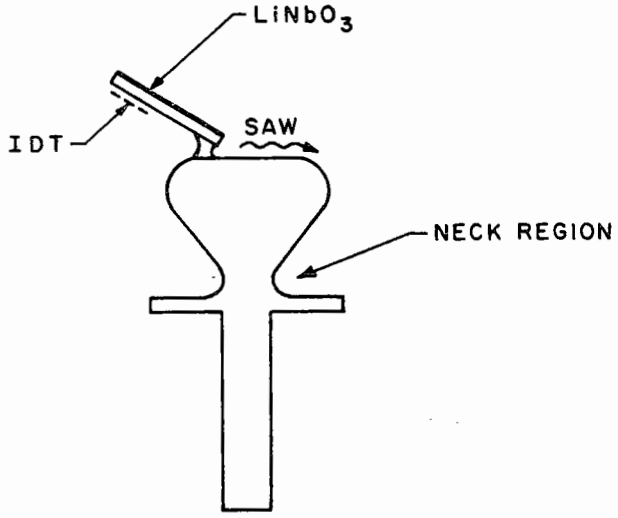

Fig. 12. Schematic of turbine blade and experimental set-up.

To determine whether there were cracks present under the machining marks, we had the neck region of the blade polished and then re-did the acoustic measurements. A picture of the neck region after polishing is shown in Fig. 13B. The subsequent acoustic study did indeed indicate the presence of cracks in the blade neck regions. Examples of the reflected echoes received in the presence and absence of cracks are shown in Figs. 14A and 14B, respectively.

CONCLUDING REMARKS

In the low frequency regime, we have found that we can detect and size cracks on flat surfaces down to crack radii of about 50 μm. From our estimates of the crack dimensions, we are then able to predict the fracture stress of a sample with a crack in it to well within 16% of the actual value.

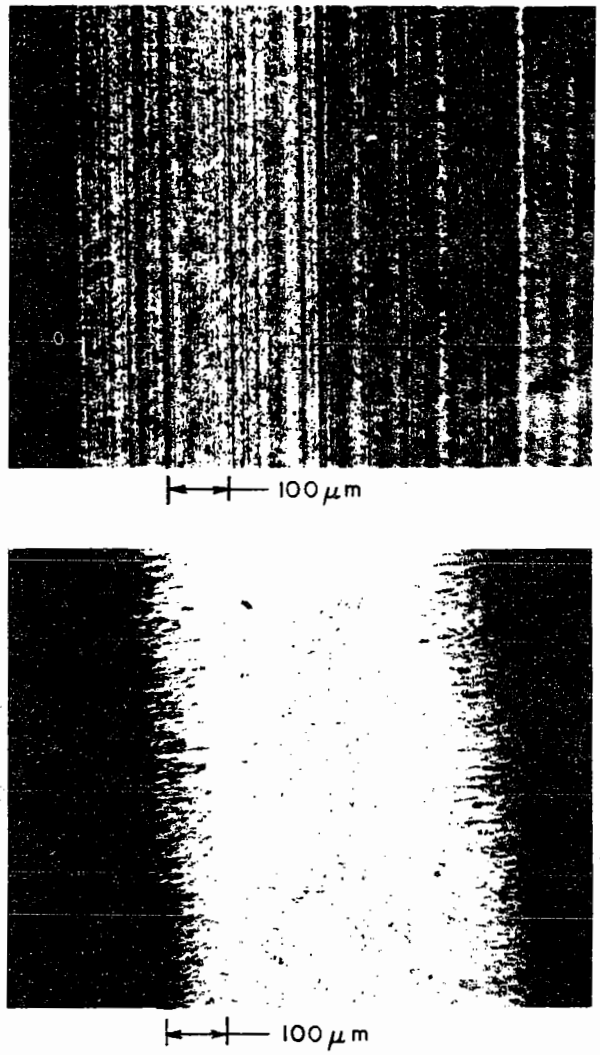

Fig. 13. Optical microscope photographs of turbine blade neck (A) before and (B) after polishing.

Cracks with radii smaller than 50 μm we find can easily be detected with higher frequency transducers. In regard to our measurements on turbine blades in this frequency regime, we are not yet able to make a good quantitative estimate of the crack size due to the presence of machining marks and corners along the propagation path as well as the complications of propagation along a curvilinear surface. To aid in quantifying our measurements here, we thus propose to introduce in the neck region of the blades half-penny shaped cracks of known size using a Knoop hardness indentor. The reflected signals from these known cracks can then be used to calibrate the reflected signals from the cracks originally present in the neck region. In our future work, we aim to apply this calibration technique as well as to extend our theory into the high frequency regime.

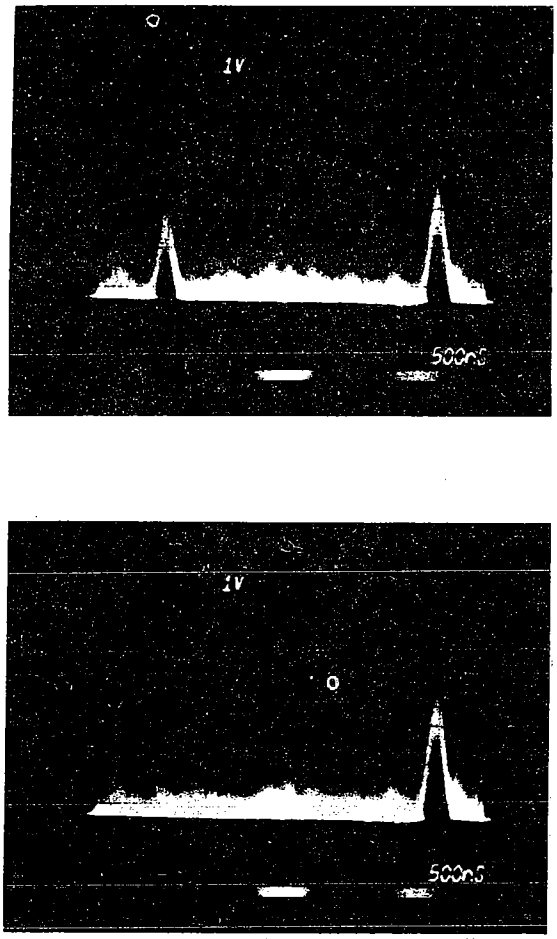

Fig. 14. Reflected echoes observed in measurements of turbine blades (A) in the presence and (B) in the absence of a crack.

ACKNOWLEDGMENT

This work was supported by the Office of Naval Research under Contract No. N00014-78-C-0283.

REFERENCES

1. G. S. Kino, "The Application of Reciprocity Theory to Scattering of Acoustic Waves by Flaws," J. Appl. Phys., vol. 49, no. 6, June 1978, pp. 3190-3199.

2. B. A. Auld, "General Electromechanical Reciprocity Relations Applied to the Calculation of Elastic Wave Scattering Coefficients," Wave Motion, vol. 1, no. 1, January 1979, pp. 3-10.

3. I. N. Sneddon, Proc. Cambridge Philos. Soc., vol. 61, 1965, p. 609.

4. B. A. Auld, Acoustic Fields and Waves in Solids, vol. II, Wiley-Interscience, New York, 1973.

5. B. Budiansky and R. J. O'Connell, "Elastic Moduli of a Cracked Solid," Int. J. Solid Structures," vol. 12, pp. 81-97, Pergamon Press, 1976.

6. F. W. Smith, A. F. Emery, and A. S. Kobayashi, "Stress Intensity Factors for Semicircular Cracks: Part 2, Semi-Infinite Solid," J. Appl. Mech. vol. 34, no. 4, pp. 953-959, December 1967.

7. I. A. Viktorov, Rayleigh and Lamb Waves, Physical Theory and Applications, Chap. 1, Plenum Press, New York, 1967.

8. M. T. Resch, B. T. Khuri-Yakub, G. S. Kino, and J. C. Shyne, "The Acoustic Measurement of Stress Intensity Factors," Appl. Phys. Lett., vol. 34, no. 3, pp. 182-184, 1 February 1979.

9. B. Budiansky and J. R. Rice, "On the Estimation of a Crack Fracture Parameter by Long-Wavelength Scattering," J. Appl. Mech., vol. 45, no. 2, pp. 453-454, June 1978.

10. J. J. Petrovic, L. A. Jacobson, P. K. Talty, and A. K. Vasudevan, "Controlled Surface Flaws in Hot-Pressed Si_3N_4," J. Amer. Ceramic Soc., vol. 58, pp. 113-116, March/April 1975.